Frequency Tuning of Third-Order Distributed Feedback Terahertz Quantum Cascade Lasers by SiO_2 and PMMA

Behnam Mirzaei, Darren Hayton, David Thoen, Jian-Rong Gao, Tsung-Yu Kao, Qing Hu, *Fellow, IEEE*, and John L. Reno

***Abstract*—We report an extensive study of the effect of an additional dielectric layer on the frequency of terahertz quantum cascade lasers (QCLs). QCLs with third-order distributed feedback structure at frequencies of 3.5 and 4.7 THz are used in our experiment. The applied dielectric layer is either Silicon dioxide (SiO_2) or Polymethylmethacrylaat (PMMA). We find that both dielectric layers can shift the lasing frequency by up to −6 GHz on a 3.5-THz QCL, and up to −13 GHz for a 4.7-THz QCL. Full 3-D FEM simulations suggest that the effect is dominated by the effective thickness of the dielectric on the side walls of the laser structure, and also confirm that for a given dielectric layer, the effect is stronger in the 4.7-THz QCL due to its different extension of the electromagnetic field to the free space. This study provides a guideline for shifting the frequency of an existing QCL for frequency critical applications such as spectroscopy or use as a local oscillator.**

***Index Terms*—Frequency tuning, local oscillator, quantum cascade laser (QCL), terahertz (THz).**

I. Introduction

TERAHERTZ (THz) quantum cascade lasers (QCLs) have been demonstrated as local oscillators for high-resolution spectroscopy both in the lab [1] and in a real astronomic instrument [2]. In the past decade, enormous progress has been made on the operating temperature [3], output power [4], beam pattern, single-mode emission [5], [6], and frequency tuning [7]–[10]. One example is the third-order distributed feedback laser [7] based on a metal–metal waveguide structure [11], which can be operated practically above 40 K using a compact low-power stirling cooler, with a targeted single-mode emission in combination with reasonable output power (∼0.5 mW) and single spot far-field beam pattern. However, due to the limited accuracy of the lithography, the difficulties to determine effective refractive index, the limited electric tuning capability, and the limited intermediate frequency bandwidth of a practical mixer [1], an additional frequency tuning possibility for a given QCL using an external dielectric layer would be extremely useful. Such a demand is justified by the fact that producing a high-quality third-order DFB QCL is inherently a costly and time-consuming process, because of the requirement for molecular beam epitaxial (MBE) growth and complex multilayer structure of the QCLs.

Continually tuning the frequency of a QCL by condensing Nitrogen gas on the laser surface at a cryogenic temperature has been reported [12], and it confirmed this unique property in a laboratory environment. However, for certain applications requiring long-term stability, such as the instrumentation in a space-like environment, alternatives are essential. In this paper, we have performed an extensive study of the effect of the dielectric layers of SiO_2 and PMMA on the shift of the lasing frequency. The advantage of the latter is its reversibility, namely the dielectric is removable. By applying full 3-D FEM simulations, we identify the importance of the thickness of the dielectric layer on the walls of the laser mesa-structure. Furthermore, we observe a stronger effect of the frequency shift in the 4.7-THz QCL than in the 3.5-THz QCL, which is supported by the simulation.

II. QCLs and Dielectric Layers Used

We use third-order DFB THz QCLs with GaAs/AlGaAs active regions based on four-well resonant phonon depopulation scheme [13], at two different frequencies of 3.5 and 4.7 THz. A schematic of a third-order QCL is shown in Fig. 1(a). All the lasers used in this study are based on the MBE structures grown at Sandia National Laboratories, but designed and fabricated at MIT. The 3.5-THz QCLs consist of 27 periods over about 1.06 mm in length, with 40 μm in width, and 10 μm in height, while the 4.7-THz QCLs have 21 periods over a length of about 0.55 mm, with a narrower width of 17 μm, and the same height

Manuscript received May 2, 2016; revised August 22, 2016; accepted September 14, 2016. Date of publication October 13, 2016; date of current version November 1, 2016. The work in The Netherlands was supported by NWO and NATO SFP. The work at MIT was supported by NASA and NSF. The work at Sandia was performed, in part, at the Center for Integrated Nanotechnologies, a U.S. Department of Energy, Office of Basic Energy Sciences user facility. Sandia National Laboratories is a multiprogram laboratory managed and operated by the Sandia Corporation, a wholly owned subsidiary of the Lockheed Martin Corporation, for the U.S. Department of Energy National Nuclear Security Administration under Contract DE-AC04-94AL85000.

B. Mirzaei and D. Thoen are with the Kavli Institute of Nanoscience, Delft University of Technology, Delft 2628, The Netherlands (e-mail: b.mirzaei@tudelft.nl; d.j.thoen@tudelft.nl).

D. Hayton is with the SRON Netherlands Institute for Space Research, Utrecht 3584, The Netherlands (e-mail: d.j.hayton@sron.nl).

J.-R. Gao is with the SRON Netherlands Institute for Space Research, Utrecht 3584, The Netherlands, and also with the Kavli Institute of Nanoscience, Delft University of Technology, Delft 2628, The Netherlands (e-mail: j.r.gao@tudelft.nl).

T.-Y. Kao is with LongWave Photonics LLC, Mountain View, CA 94043 USA (e-mail: wilt_kao@longwavephotonics.com).

Q. Hu is with the Department of Electrical Engineering and Computer Science and Research Laboratory of Electronics, Massachusetts Institute of Technology, Cambridge, MA 02139 USA (e-mail: qhu@mit.edu).

J. L. Reno is with Sandia National Laboratories, Albuquerque, NM 87185-0601 USA (e-mail: jlreno@sandia.gov).

Color versions of one or more of the figures in this paper are available online at http://ieeexplore.ieee.org.

Digital Object Identifier 10.1109/TTHZ.2016.2613519

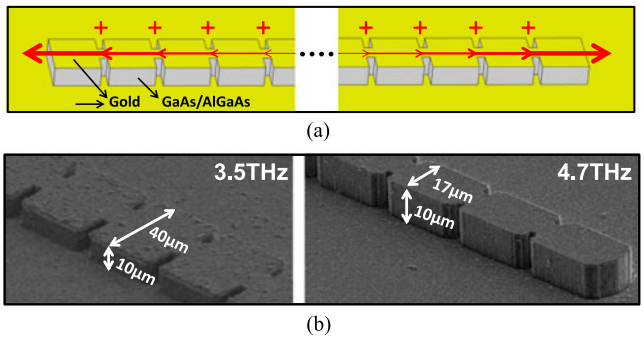

Fig. 1. (a) Schematic of the third-order DFB QCL general geometry, and principle, and THz radiation emission. (b) SEM photographs of our experimental 3.5-THz (left) and 4.7-THz (right) QCLs, consisting of 27 periods of ∼40 μm long and 21 periods of ∼27 μm long, respectively.

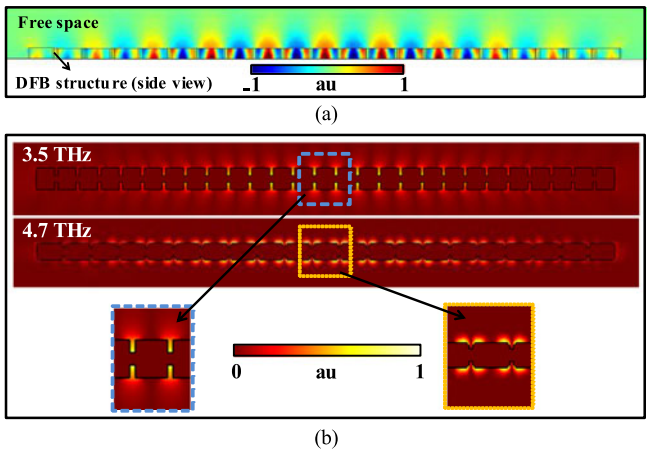

Fig. 2. (a) Side view of the normalized electric field in the DFB structure of 4.7-THz QCL and free space, which constructively interferes for the main mode. (b) Top view of the normalized magnitude of the extending electric field to the free space for 3.5-THz (top) and 4.7-THz (bottom) QCLs. Close-up figures show the difference of the field distribution in both lasers.

of 10 μm. Multiple lasers are grouped together on a single chip. The SEM photographs of both laser structures are illustrated in Fig. 1(b). The tapered horn shape grating of the 4.7-THz DFB laser can make a larger radiation loss for the modes near the upper side of the grating, while reduce the radiation loss for the modes at the other side of the bandgap. The disparity comes from the difference in the relative position between the tip of the tapered horn and the peak field spots inside the laser cavity for both band edge modes. Effectively, this approach leverages a tradeoff between the output power efficiency and mode selectivity. The tip of the tapered horn is designed to be located at one third of the ridge width away from the edge of the laser ridge and the width of the horn opening is roughly 15% of the overall DFB periodicity. Based on the power measurements of similar lasers, we expect the maximum output powers of about 0.8 [1] and 0.25 mW [14] for 3.5- and 4.7-THz QCLs, respectively.

Fig. 2(a) shows a lateral profile of the electromagnetic (EM) field inside a third-order DFB waveguide, and in free space, demonstrating how they constructively interfere along the waveguide surface to make a narrow far field beam toward both directions [15], which is also shown by the arrows in Fig. 1(a). The resonant frequency f of a third-order DFB QCL is determined by the effective refractive index, $\mathrm{n_{eff}}$, through an expression $f = 3c/2\mathrm{n_{eff}}\Lambda$ where c is the speed of light in free space and Λ is the period of the grating structure (the length of the sections). So, for a given design, any changes with regard to the EM field surrounding the laser structure, for example, adding a dielectric layer, may affect $\mathrm{n_{eff}}$ and can, thus, change the frequency. This is the essence of the technique for frequency shifting to be applied in this study. To illustrate the physical principle of the changing frequency, we also include simulated electric field distributions around the DFB structures using the full 3-D FEM modeling [see Fig. 2(b)], where the field extends into the free space, originating from the lateral sides of the laser. The extended field can sense additional dielectric effectively, and, therefore, increase $\mathrm{n_{eff}}$ and consequently decrease the frequency.

As shown in Fig. 2(b), the field distribution is different in the two lasers. For the 4.7-THz QCL, it is more localized along the period edges, which increases the probability to be contacted by a deposited layer, while for 3.5-THz QCL, it is more concentrated inside and around the air gaps, making the effect weaker, since it covers a smaller portion of the entire lateral area. The effect strength mainly depends on the ratio between the wavelength and the laser width, which is larger for the 4.7-THz QCL, suggesting a larger frequency shift for this laser for the same dielectric layer. Detailed simulation of the frequency shift as a function of a dielectric layer will be described later for comparison with the experimental results.

We focus on two dielectric materials: one is SiO_2 and the other is PMMA. SiO_2 has a reasonable refractive index of ~ 2 at both frequencies of interest [16]. For our purpose, a higher index is favorable. SiO_2 also has relatively low absorption coefficients of ∼26 and 35 $\mathrm{cm^{-1}}$ [16] at frequencies of 3.5 and 4.7 THz, respectively. Although lower absorption is preferred, the dielectric layer applied is so thin that the loss is relatively small. Furthermore, use of this material is well known in nanofabrication. We deposit a layer of SiO_2 by radio-frequency (RF) sputtering at room temperature (Alliance Concept AC450) and with different thicknesses. A disadvantage however is that, after deposition, SiO_2 cannot be removed without significant risk of damage to the QCL.

PMMA is the other candidate used in this study. It has a refractive index of ∼1.54 and 1.56 at frequencies of 3.5 and 4.7 THz, respectively, but with a higher absorption coefficient of $\sim$ 50 $\mathrm{cm^{-1}}$ [17] at both frequencies. The advantage is that the PMMA can relatively easily be removed by Acetone; thus, it is always possible to return the laser to its original frequency. Due to the physical nature of these QCLs, for example, the use of wire bonds for electrical contacts, the usual spin coating deposition of PMMA is unavailable to us. Instead, we add the PMMA by placing a droplet of solvent diluted PMMA onto the laser chip and leaving it to dry in ambient conditions in the lab overnight. This forms a layer of solid PMMA covering the laser structure. This process is simple and reliable but with the disadvantage of reduced control over the resulting thickness (relative to spin coating). To reach required thickness, however, one can in principle repeat this process with different PMMA concentrations.

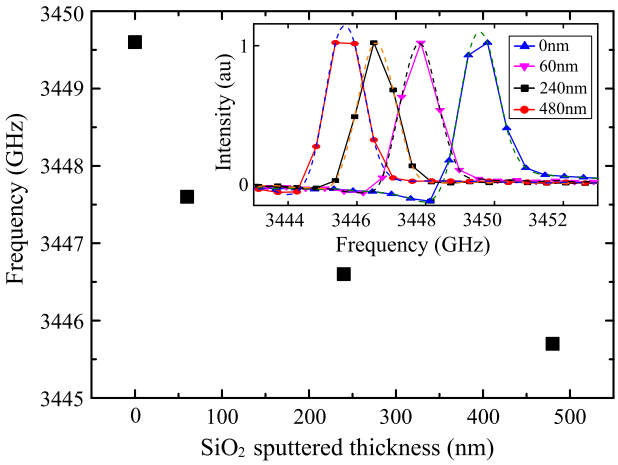

Fig. 3. Measured frequency as a function of the thickness of the sputtered SiO_2 on the 3.5-THz QCL. The thickness is zero when there is no SiO_2. Inset: Normalized measured FTS spectra without and with three different thicknesses of the sputtered SiO_2. Dashed are fitted curves to find the central frequencies.

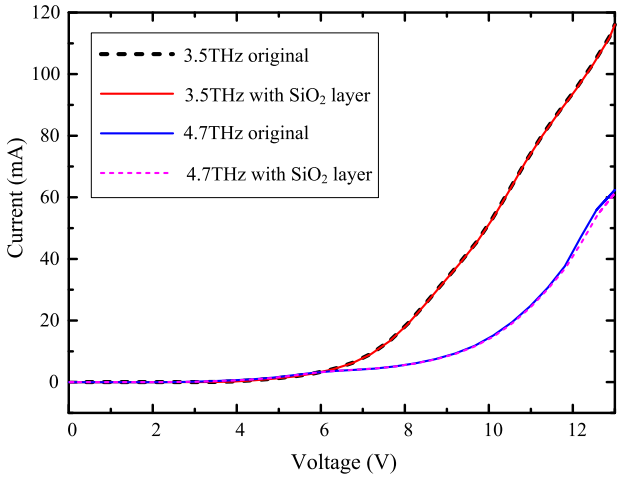

Fig. 4. Measured *I–V* curves of both lasers before and after SiO_2 deposition.

Since all lasers are fine structures with wire bond based devices, it is also prohibitive to use ultrasonic cleaning as would normally be standard prior to SiO_2 or PMMA deposition, but to avoid breaking the bonding wires and damaging metal Au layers, we clean our lasers in hot acetone.

III. Measurement Setup

We use a pulse tube cooler to operate the 3.5- and 4.7-THz QCL at temperatures of ∼10 and ∼6 K, respectively. We measure the emission spectra of a QCL before and after adding a dielectric layer using a cryogenic Silicon-bolometer-based Fourier transform spectrometer (FTS) with a resolution of ∼0.6 GHz, and an uncertainty of less than 0.1 GHz. We determine the laser central frequency by fitting the data of the measured spectral line (inset of the Fig. 3). To make the comparison possible, all the electrical biasing and temperature conditions are kept the same for a given laser in different measurements to make sure that the frequency shift is determined only by the added dielectric layer. All the measurements are performed in the normal laboratory condition (no vacuum). Due to the relatively long optical path between the QCL and the FTS, we can only select suitable lasers with a frequency well clear of strong, mainly water, absorption lines, which are abundant at these frequencies. To monitor the effect of the dielectric layer on QCL output power, we use a room temperature pyroelectric detector positioned very close to the window of the cryostat. This avoids the possibility that power measurements are affected by changes in atmospheric absorption due to frequency change.

IV. Measurement and Simulation Results

A. Results on 3.5-THz QCLs

The frequency of the 3.5-THz QCL versus the thicknesses of sputtered SiO_2, varying from 0, 60, 240, and 480 nm, is plotted in Fig. 3. The inset shows the corresponding measured, FTS spectra, together with fitted curves for accurately determining the central frequencies. The measured shifts with respect to the original frequency are −2, −3, and −3.9 GHz, respectively. The SiO_2 thickness is not measured directly from the laser, but from a flat monitor sample, positioned next to the laser during the sputtering deposition.

TABLE I
Simulations Input Parameters

Parameter	Value for 3.5-THz QCL	Value for 4.7-THz QCL
Laser width	40 μm	17 μm
Laser height	10 μm	10 μm
Period length	40 μm	27 μm
Number of periods	27	21
Slit opening length	5.8 μm	2.5 μm
SiO_2 refractive index	2	2
SiO_2 absorption coefficient	26 cm^{-1}	35 cm^{-1}
PMMA refractive index	1.54	1.56
PMMA absorption coefficient	50 cm^{-1}	50 cm^{-1}

We assume that the measured thickness is the same as one on the top and substrate of the laser, which is referred to the surface layer thickness [blue color part in Fig. 5(b)]. Although the more down shift is observed when the thickness of SiO_2 increases, we observe almost no effect on the output power in comparison with the original value even when the 480-nm-thick SiO_2 is added.

We also measured the *I–V* curves of the lasers before and after deposition (shown in Fig. 4), which show a negligible difference. This indicates that the operation properties of the lasers are kept unchanged.

To understand the measured thickness dependence, we perform full 3-D FEM simulations using COMSOL 5.1. We take the DFB waveguide structure with the same parameters as the actual laser used, and do the eigenfrequency study in the RF module to find the resonant frequency. There we can add whatever material with known characteristics, around the structure, and find the effect on the resonance frequency. Input parameters used in simulations are summarized in the Table I.

To obtain the thickness of the SiO_2, it is less straight forward. This is because we only know the surface layer thickness, but

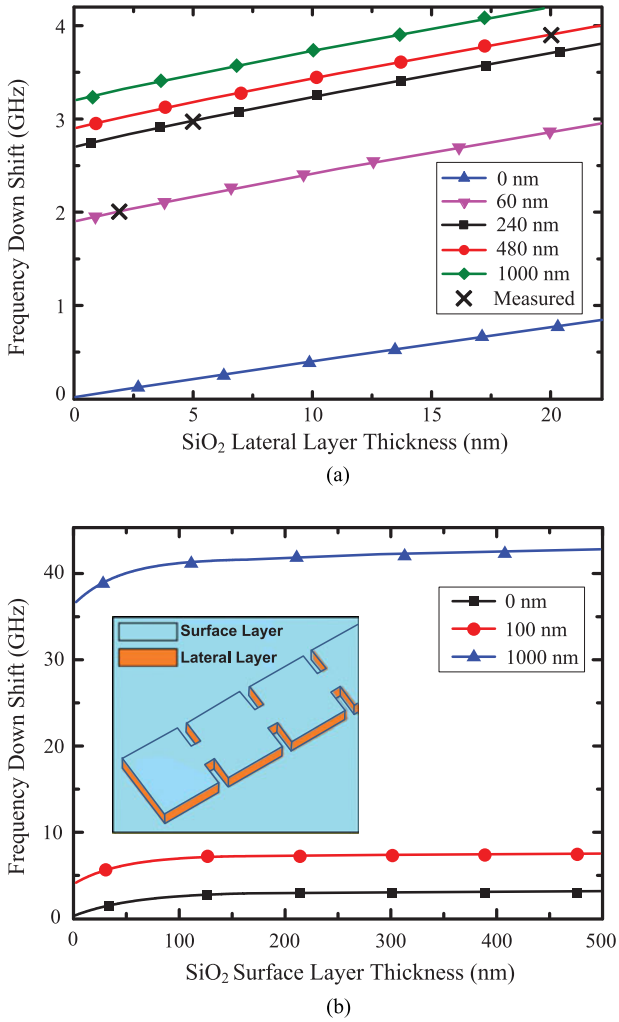

Fig. 5. (a) Simulation results of the frequency down shift for the 3.5-THz QCL versus the lateral layer thickness of the sputtered SiO_2, in different surface layer thicknesses, together with the measured data. (b) Simulated frequency downshift versus surface layer thickness of SiO_2 on a 3.5-THz QCL, in different lateral layer thicknesses. Inset: demonstration of the surface and lateral layers.

not the layer thickness on the walls of the waveguide structure [lateral layer thickness, the area shown in orange in Fig. 5(b)], which can depend on the details of the sputtering process and also of the surface condition of the laser before the deposition. However, it is a common knowledge that the lateral thickness should be smaller and even considerable smaller than the surface thickness in a practical sputtering deposition. To establish the frequency shift as a function of the lateral layer thickness, we simulate it for different surface thicknesses of SiO_2 on the 3.5-THz QCL including our measured points at 60, 240, and 480 nm. The results are plotted in Fig. 5(a). Based on the calculated dependences, we find that the lateral thicknesses in our case are ~2, 5, and 20 nm, respectively, by matching the calculated frequency shift to the measured one.

Fig. 5(a) shows that the frequency shift has approximately a linear dependence to the lateral layer thickness with a rate of ~40 MHz/nm for a fixed surface layer thickness around our experimental values. As it is shown in Fig. 5(b), above a certain range of the initial surface layer thickness (~100 nm) where the effect is larger, the shift is mainly determined by the lateral layer thickness, while the effect due to changing the surface layer thickness in the same scale is negligible. In that region, it shows an almost linear dependence to the surface layer thickness with a coefficient of ~ 1 MHz/nm. We made this graph based on the simulated data points down to 60 nm of the surface layer thickness and the rest down to zero is made by fitting. That initial nonlinear region also implies that the EM field is being rapidly attenuated by the vertical distance from the top surface, while in the lateral sides, it remain almost unchanged over ~1 μm away from the wall surface.

Alternatively, we apply a layer of PMMA as the dielectric layer on a different 3.5-THz laser that has the same structure as the one used previously with SiO_2. A shift of ~-6.3 GHz is observed experimentally. In contrast to the case of using SiO_2, a drop of ~18% in the output power is observed (from 0.8 to 0.58 mW), which is consistent with the higher absorption of PMMA. The reduction of the output power may also suggest a much thicker layer of PMMA than the SiO_2 used so far. As explained in the previous section, for PMMA deposition, it is difficult to accurately control the thickness. On the laser, it is technically challenging to measure the thickness. However, we think the layer distribution, in comparison with the sputtered SiO_2 with poor wall coverage, can be different. Since the liquid PMMA covers the laser, evaporating very slowly, it is reasonable to assume that the QCL is homogeneously covered by PMMA on the surface and also on the walls of the laser structure. With this assumption, we can analyze the measurement by applying 3-D simulations.

We calculate the frequency shift of the 3.5-THz laser as a function of the PMMA thickness. The dependence is plotted in Fig. 6(b), together with the experimental data point by matching the frequency shift. We derive the thickness of PMMA to be 340 nm in our case.

The calculated down shift as a function of PMMA thickness allows an estimate of the frequency shift rate, which is nearly constant and is about 10 MHz/nm. The shift rate, being a factor of 4 lower than that found in the SiO_2 simulation, is due to the lower refractive index of PMMA (~1.54) compared to SiO_2 (~2). In addition, a higher absorption coefficient, that attenuates the EM field more strongly as it enters into the PMMA layer, can reduce the influence of the layer on the effective refractive index of the laser.

B. *Results on 4.7-THz QCLs*

Now we describe experiments to add a similar dielectric layer to 4.7-THz QCLs. The frequency of these QCLs is motivated by the development of heterodyne receivers to observe the astronomically important neutral oxygen [OI] line at 4.745 THz. We start with a relatively fresh 4.7-THz QCL, like the 3.5-THz QCLs used, by sputter growing a layer of 410-nm SiO_2 on the surface and found a frequency shift of ~ −13.3GHz, which seems to have a much stronger effect than what we observed for the 3.5-THz QCL (nearly three times larger down shift for a comparable thickness of SiO_2). Before describing the simulation, we also noticed that the output power after the deposition

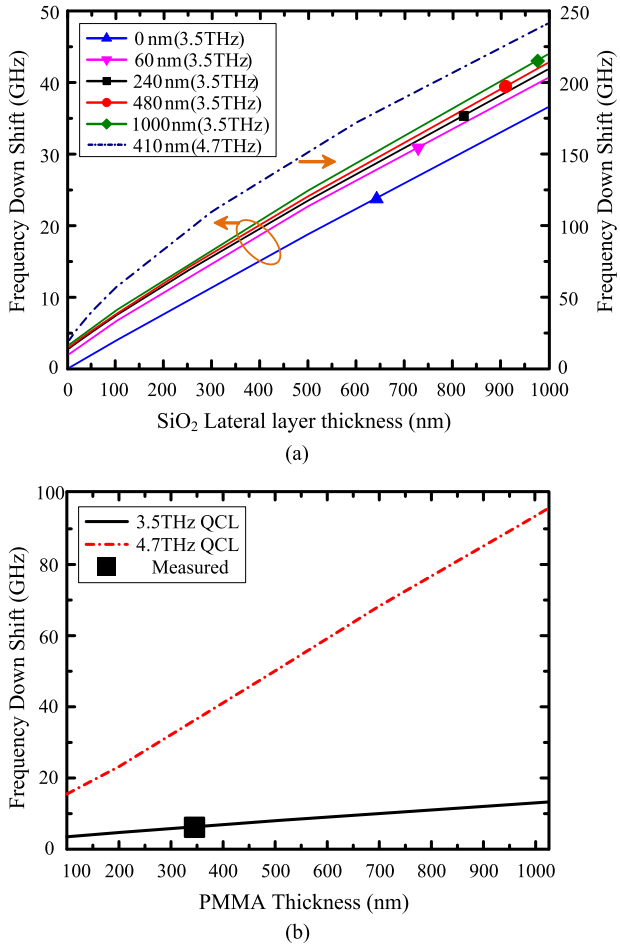

Fig. 6. (a) Simulation results of the frequency down shift of the 3.5-THz QCL versus the lateral layer thickness of the sputtered SiO_2, up to 1 μm, in different surface layer thicknesses, and the same curve for the 4.7-THz QCL with the measured surface thickness of 410 nm. (b) Simulated frequency down shift of the 3.5-THz QCL and also the 4.7-THz QCL as a function of PMMA layer thickness, which are assumed to be coated uniformly across the laser structure.

of SiO_2 had a reduction of about 20%. This may be partly due to the increased absorption loss in the SiO_2 at this frequency [16], and may be partly due to the fact that the EM field is more strongly interacting with the added material, as expected from the simulation result shown in Fig. 2(b).

To understand the result obtained with the 4.7-THz QCL, we have repeated the simulation using the 3-D simulator in COMSOL with the input parameters adjusted to match the actual QCL. The down shift of the frequency as a function of the lateral layer thickness for the surface layer thickness of 410 nm is shown in Fig. 6(a). To derive the lateral thickness, we try to match the down shift in the simulated curve where we find that the experimental data point does not fit. In other words, even with zero lateral thickness used in the simulation, we already have a larger down shift than had been observed experimentally. We attributed these results to the problematic surface condition of this laser, which is different from that of the 3.5-THz QCL. The unknown surface condition can reduce the effect of the dielectric on the frequency in two ways: it may absorb considerably the EM field, reducing the effect of additional SiO_2 or PMMA layer, and it prevents them to adhere on the walls of the laser structure.

We have also performed the same experiments using a second 4.7-THz QCL, which has been frequently tested experimentally so far, and is known to suffer from surface contamination. We have sputtered SiO_2 and also applied PMMA to this laser, however, we observe a weaker effect, not more than -3-GHz shift which confirms the crucial role of the laser surface condition. It is worth to stress that we do perform the normal cleaning procedure using acetone, but it seems to be not as effective at cleaning-up severe contamination in our case. Applying more aggressive cleaning techniques like Oxygen plasma or acetone with ultrasound agitation is not applicable because of the potential to damage the lasers.

Comparing to the same graphs of the frequency down shift versus deposited SiO_2 lateral layer thickness, for the 3.5-THz QCL in Fig. 6(a), the simulation result for 4.7-THz QCL shows much larger effect, characterized by a rate of 200 $\mathrm{MHz/nm}$. It confirms the intuitive estimation by taking the different outward extended EM distribution of a 4.7-THz QCL into account. This is also confirmed by the simulation for the effect of a homogeneous PMMA layer on a 4.7-THz QCL, plotted in Fig. 6(b), where it shows a coefficient around 88 MHz/nm, being more than eight times larger comparing to the 3.5-THz laser.

C. Discussion

The experimental results from the 3.5-THz QCL show that with a layer of sputtered SiO_2, one can down shift the frequency of the laser. It also shows that with the simulations, the effect of the lateral layer thickness of the SiO_2 is dominated comparing to the surface layer thickness. The typical frequency shift rate is about $-$ 40 MHz/nm. Knowing this, one can try to sputter a layer of SiO_2 when the laser is positioned with an angle (or tilted), so that the material can more effectively be deposited on the side walls instead of on the top of the laser. If the surface thickness of SiO_2 is not far from 500 nm, the loss is still negligible, so the output power is affected minimally. The dielectric layer based on PMMA is easily introduced. As we have shown, a -6-GHz frequency shift can be realized with negligible power loss. This approach offers a reversible process, so one can always remove the PMMA to recover the original frequency. It is interesting to note that during limited thermal cycling of the QCL with PMMA, we do not see the change with regard to the frequency.

We have performed an extensive study on the effect of SiO_2 and PMMA on the frequency shift of third-order DFB QCLs at 3.5 THz. We, however, can present only a few experimental data points since we have limited number of QCLs available for such experiments which are uniquely designed to be served as local oscillators in certain space applications. Nevertheless, we confirm and establish the frequency dependence on the additional dielectric layers of sputtered SiO_2 and PMMA in combination with the 3-D simulation.

Although the simulation for the 4.7-THz QCLs is informative itself, it is unable to match the experimental result because of the problematic laser surface condition, e.g., contamination. However, as a by-product, we realize that the surface condition of the laser before the deposition of SiO_2 is crucial and the fresh

lasers are preferable for the change of the frequency by such a technique. The measured frequency shift of about −13 GHz together with the simulation results shows that the 4.7-THz QCL due to the strong extension of the EM field to the free space is more sensitive to the presence of a dielectric layer as well as the presence of the contamination. In practice, we have observed measurable down shifts due to the contamination caused, for example, by an oil pumping system. So, to maintain the frequency of as-produced QCL, one should prevent the contamination.

V. Conclusion

We have extensively studied the frequency down shift of third-order DFB QCLs at 3.5 THz as a function of the thickness of a dielectric layer of either sputtered SiO_2 or PMMA. We observed that both materials can effectively down shift the lasing frequency. Taking advantage of the 3-D FEM simulations, we study the frequency dependence on the layer thickness both on the flat surfaces and lateral sides of the structure, where we realize that the latter dominates the frequency shift. SiO_2 is recommended when a high down shift with high accuracy is desired, while PMMA is the choice if the frequency shift has to be reversible since it is easily removable. The knowledge provides a guideline to shift the frequency of an existing QCL used as a local oscillator in practical applications. We have performed a similar study also on the third-order DFB QCLs at 4.7 THz and observed a larger frequency shift, supporting the prediction of the 3-D FEM simulation. However, due to the surface contamination, no consistent experimental dependence was established.

Acknowledgment

Author B. Mirzaei acknowledges the support and encouragement from L. Kouwenhoven. The authors would also like to thank W. Laauwen at SRON for his inputs and discussions and E. E. Orlova for her comments.

References

[1] J. L. Kloosterman *et al.*, "Hot electron bolometer heterodyne receiver with a 4.7-THz quantum cascade laser as a local oscillator," *Appl. Phys. Lett.*, vol. 102, pp. 011123-1–011123-4, 2013.

[2] H. Richter, M. Wienold, L. Schrottke, K. Biermann, H. T. Grahn, and H. W. Hubers, "4.7-THz local oscillator for the GREAT heterodyne spectrometer on SOFIA," *IEEE Trans. THz Sci. Technol.*, vol. 5, no. 4, pp. 539–545, Jul. 2015.

[3] S. Fathololoumi *et al.*, "Terahertz quantum cascade lasers operating up to ∼200K with optimized oscillator strength and improved injection tunneling," *Opt. Exp.*, vol. 20, pp. 3866–3876, 2012.

[4] M. Brandstetter *et al.*, "High power terahertz quantum cascade lasers with symmetric wafer bonded active regions," *Appl. Phys. Lett.*, vol. 103, pp. 171113-1–171113-5, 2013.

[5] M. I. Amanti, G. Scalari, F. Castellano, M. Beck, and J. Faist, "Low divergence terahertz photonic-wire laser," *Opt. Exp.*, vol. 18, pp. 6390–6395, 2010.

[6] T. Y. Kao, Q. Hu and J. L. Reno, "Perfectly phase-matched third-order distributed feedback terahertz quantum-cascade lasers," *Opt. Lett.*, vol. 37, no. 11, pp. 2070–2072, 2012.

[7] Q. Qin, B. S. Williams, S. Kumar, J. L. Reno, and Q. Hu, "Tuning a terahertz wire laser," *Nature Photon.*, vol. 3, pp. 732–737, 2009.

[8] J. Xu *et al.*, "Tunable terahertz quantum cascade lasers with an external cavity," *Appl. Phys. Lett.*, vol. 91, pp. 121104-1–121104-3, 2007.

[9] F. Castellano *et al.*, "Tuning a microcavity-coupled terahertz laser," *Appl. Phys. Lett.*, vol. 107, pp. 261108-1–261108-5, 2015.

[10] D. Turcinkova, M. I. Amanti, G. Scalari, M. Beck, and J. Faist, "Electrically tunable terahertz quantum cascade lasers based on a two-sections interdigitated distributed feedback cavity," *Appl. Phys. Lett.*, vol. 106, pp. 131107-1–131107-4, 2015.

[11] B. S. Williams, S. Kumar, H. Callebaut, Q. Hu, and J. L. Reno, "Terahertz quantum-cascade laser at $\lambda \approx 100\,\mu$m using metal waveguide for mode confinement," *Appl. Phys. Lett.*, vol. 83, pp. 2124–2126, 2003.

[12] D. Turčinková, M. I. Amanti, F. Castellano, M. Beck, and J. Faist, "Continuous tuning of terahertz distributed feedback quantum cascade laser by gas condensation and dielectric deposition," *Appl. Phys. Lett.*, vol. 102, pp. 181113-1–181113-4, 2013.

[13] B. S. Williams, S. Kumar, Q. Hu, and J. L. Reno, "Resonant phonon terahertz quantum-cascade laser operating at 2.1 THz ($\lambda \approx 141\,\mu$m)," *Electron. Lett.*, vol. 40, pp. 431–433, 2004.

[14] Y. Ren *et al.*, "Frequency and amplitude stabilized terahertz quantum cascade laser as local oscillator," *Appl. Phys. Lett.*, vol. 101, pp. 101111-1–101111-4, 2012.

[15] N. van Marrewijk *et al.*, "Frequency locking and monitoring based on bi-directional terahertz radiation of a third-order distributed feedback quantum cascade laser," *J. Infrared Millimeter THz Waves*, vol. 36, pp. 1210–1220, 2015.

[16] E. D. Palik, *Handbook of Optical Constants of Solids*. Orlando, FL, USA: Academic Press, 1985, p. 753.

[17] P. D. Cunningham *et al.*, "Broadband terahertz characterization of the refractive index and absorption of some important polymeric and organic electro-optic materials," *J. Appl. Phys.*, vol. 109, pp. 043505-1–043505-5, 2011.

Behnam Mirzaei received the M.Sc. degree in electrical engineering from the University of Tabriz, Tabriz, Iran, in 2009, and is currently working toward the Ph.D. degree at the Delft University of Technology, Delft, The Netherlands.

Since 2014, he has been with the Delft University of Technology, working on terahertz quantum cascade lasers as local oscillators for space applications.

Darren Hayton was born in Worcestershire, U.K. He received the B.Sc. degree in planetary and space physics and the Ph.D. degree in semiconductor characterization from the University of Wales, Aberystwyth, Cardiff, U.K., in 1998 and 2002, respectively. The title of his Ph.D. was "Spectroscopic Ellipsometry of Solids" and focused on developing a nondestructive characterization technique for semiconductor bulk/oxide interface layers in SiC.

He has been a Postdoctoral Researcher in the field of terahertz detector and detector systems development with the Astronomy Instrumentation Group, Cardiff University, Cardiff, U.K., and with the Astronomical Instrumentation Group, University of Lethbridge, Lethbridge, AB, Canada. He is currently an Instrument Scientist with the SRON Netherlands Institute for Space Research, Utrech, The Netherlands, where his research interests include terahertz and superterahertz hot electron bolometer (HEB) heterodyne mixer receivers for astronomy, quantum cascade lasers (QCL) as terahertz local oscillator sources for HEB and phase-/frequency-locking techniques for QCL systems based on superlattice harmonic mixing.

David Thoen was born in Nieuwveen, The Netherlands, in 1978. He received the B.Sc. degree in applied physics from the Fontys University of Technology, Eindhoven, The Netherlands, in 2008.

He started in 2007 as a Microwave Engineer with the Dutch Institute for Fundamental Energy Research (formerly known as the FOM Institute Rijnhuizen), Nieuwgein. The Netherlands, working on microwave diagnostics for real-time control of electron-cyclotron resonance heating of nuclear fusion plasmas in tokamaks. In 2010, he joined the Cosmo Nanoscience Group, Delft University of Technology, Delft, The Netherlands, working on the development and fabrication of the band 9 (600–720 GHz) detector chips of the Atacama Large Millimeter Array. Since 2012, he has been working on microwave kinetic inductance detectors, from 2015, with the Terahertz Sensing Group, Delft University of Technology. He is responsible for the MKID processing in the Kavli cleanroom at Delft with a focus on reactive sputtering of niobium-titanium-nitride and quality control of thin films. He has co-authored more than 20 papers.

Jian-Rong Gao was born in Shanghai, China, in 1959. He received the B.Sc. and M.Sc. degrees in physics from Fudan University, Shanghai, in 1982 and 1985, respectively, and the Ph.D. degree from Delft University of Technology (TU Delft), Delft, The Netherlands, in 1991.

He continued to do his Postdoctorate research with the University of Groningen, Groningen, The Netherlands. He is a Senior Instrument Scientist with the SRON Netherlands Institute for Space Research, Utrecht, The Netherlands, and Groningen and also, through a SRON-TU Delft research contract, serves as a part time staff member with the Kavli Institute of Nanoscience and Delft Space Institute, TU Delft. He has authored or co-authored approximately 240 publications. His prime interests include superconducting detectors, semiconductor terahertz sources, and instrumentation for balloon and space applications. His research interests include terahertz SIS mixers, HEB mixers, KIDs, TES for both FIR and X-ray detection, and terahertz quantum cascade lasers as local oscillators.

Tsung-Yu Kao received the B.S. degree in electrical engineering and physics from National Taiwan University, Taipei, Taiwan, in 2005, and the M.Sc. and Ph.D. degrees in electrical engineering from the Massachusetts Institute of Technology, Massachusetts, CA, USA, in 2009 and 2013, respectively. His Ph.D. research interests include high-power terahertz DFB laser arrays and terahertz amplifiers.

He joined LongWave Photonics LLC, Mountain View, CA, USA, the first terahertz QC laser provider in the world, as CTO in 2014. He has co-authored more than 20 papers published in peer-reviewed journals, such as the *APL*, *Optics Letters*, and *Nature Photonics*.

Qing Hu (M'03–SM'03–F'10) received the Ph.D. degree in physics from Harvard University, Cambridge, MA, USA, in 1987.

From 1987 to 1989, he was a Postdoctoral Associate with the University of California at Berkeley, Berkeley, USA. He joined the Massachusetts Institute of Technology, Cambridge, in 1990, where he is currently a Distinguished Professor with the Electrical Engineering and Computer Science Department. He has made significant contributions to physics and device applications over a broad electromagnetic spectrum from millimeter wave, terahertz (THz), to infrared frequencies. Among those contributions, the most distinctive is his development of high-performance THz quantum cascade lasers. Now this breakthrough has already found applications in heterodyne receiver technology and real-time THz imaging, which was also pioneered by his group.

Dr. Hu is a Fellow of the Optical Society of America (OSA), a Fellow of the American Physical Society, and a Fellow of the American Association for the Advancement of Science. He was the recipient of the 2012 IEEE Photonics Society William Streifer Scientific Achievement Award and the 2015 Nick Holonyak, Jr., Award from the OSA. He has been an Associate Editor of *Applied Physics Letters* during 2006–2014 and has been a Deputy Editor since 2015.

John L. Reno is an expert on Molecular Beam Epitaxy (MBE) growth. He is a part of the Center for Integrated Nanotechnologies, Sandia National Laboratories, Albuquerque, NM, USA. Prior to his current work, he has performed MBE growth of a wide range of materials including HgCdTe, widegap II–VI materials, high Tc superconductors, narrow gap group IV materials, and short-period superlattices on InP. His primary research interests include high-purity nanostructured electronic materials, with an emphasis on the synthesis of AlGaInAs-based materials. His current research interests include intersubband transitions and high-mobility heterostructures, quantum cascade lasers in the terahertz and infrared range, quantum well infrared photodetectors, high-mobility materials for low-dimensional quantum transport studies, and the study of the interaction between semiconductor materials and metamaterial for new optical applications.